Novel bisnaphthalimidopropyl (BNIPs) derivatives as anticancer compounds targeting DNA in human breast cancer cells.

KOPSIDA, M., BARRON, G.A. BERMANO, G., KONG THOO LIN, P. and GOUA, M.

2016

Organic & Biomolecular Chemistry

PAPER

View Article Online
View Journal | View Issue

Cite this: *Org. Biomol. Chem.*, 2016, **14**, 9780

Novel bisnaphthalimidopropyl (BNIPs) derivatives as anticancer compounds targeting DNA in human breast cancer cells†

Maria Kopsida,[a] Gemma A. Barron,[a,b] Giovanna Bermano,[b] Paul Kong Thoo Lin[a] and Marie Goua*[a]

Bisnaphthalimidopropyl (BNIP) derivatives are a family of compounds that exert anti-cancer activities *in vitro* and, according to previous studies, variations in the linker sequence have increased their DNA binding and cytotoxic activities. By modifying the linker sequence of bisnaphthalimidopropyl diaminodicyclohexylmethane (BNIPDaCHM), a previously synthesised BNIP derivative with anti-cancer properties, three novel BNIP derivatives were designed. Bisnaphthalimidopropyl-piperidylpropane (BNIPPiProp), a structural isomer of BNIPDaCHM, bisnaphthalimidopropyl ethylenedipiperidine dihydrobromide (BNIPPiEth), an isoform of BNIPDaCHM with a shorter linker chain, and (*trans*(*trans*))-bisnaphthalimidopropyl diaminodicyclohexylmethane (*trans*,*trans*-BNIPDaCHM), a stereoisomer of BNIPDaCHM, were successfully synthesised (72.3–29.5% yield) and characterised by nuclear magnetic resonance spectroscopy (NMR) and mass spectrometry (MS). Competitive displacement of ethidium bromide (EtBr) and UV binding studies were used to study the interactions of BNIP derivatives with *Calf Thymus* DNA. The cytotoxicity of these derivatives was assessed against human breast cancer MDA-MB-231 and SKBR-3 cells by MTT assay. Propidium iodide (PI) flow cytometry was conducted in order to evaluate the cellular DNA content in both breast cancer cell lines before and after treatment with BNIPs. The results showed that all novel BNIPs exhibit strong DNA binding properties *in vitro*, and strong cytotoxicity, with IC_{50} values in the range of 0.2–3.3 μM after 24 hours drug treatment. Two of the novel BNIP derivatives, BNIPPiEth and *trans*,*trans*-BNIPDaCHM, exhibited greater cytotoxicity against the two breast cancer cell lines studied, compared to BNIPDaCHM. By synthesising enantiopures and reducing the length of the linker sequence, the cytotoxicity of the BNIP derivatives was significantly improved compared to BNIPDaCHM, while maintaining DNA binding and bis-intercalating properties. In addition, cell cycle studies indicated that *trans*,*trans*-BNIPDaCHM, the most cytotoxic BNIP derivative, induced sub-G1 cell cycle arrest, indicative of apoptotic cell death. Based on these findings, further investigation is under way to assess the potential efficacy of *trans*,*trans*-BNIPDaCHM and BNIPPiEth in treating human breast cancer.

Received 23rd August 2016,
Accepted 21st September 2016

DOI: 10.1039/c6ob01850e

www.rsc.org/obc

Introduction

Breast cancer is the most commonly occurring cancer in women, with incidence rates approaching 1.38 million cases per year worldwide.[1] Breast cancer, depending on whether it develops in response to the hormone oestrogen, is divided in two categories: oestrogen dependent (ER^+) and oestrogen independent (ER^-) cancer.[2] ER^+ breast cancers respond better to anti-oestrogen (endocrine) therapies, such as tamoxifen and exemestane, by inhibiting the effect of oestrogen and decreasing the uncontrolled proliferation of breast cancer cells.[2] On the other hand, ER-breast cancers are more invasive and less responsive to current standard-of-care treatment regimes, such as fluorouracil, epirubicin and doxorubicin, which do not selectively target breast cancer cells hence leading to severe side effects.[3] Over the last few decades, there have been numerous attempts to develop novel breast cancer-specific therapies that will act on specific molecular targets, increasing selectivity and potentially reducing treatment resistance and side effects.[4] DNA was one of the first biochemical targets identified in anti-cancer therapeutics,[5–7] which lead to a new

[a]*School of Pharmacy and Life Sciences, Robert Gordon University, Garthdee Road, Aberdeen, AB10 7GJ Scotland, UK. E-mail: m.goua@rgu.ac.uk*
[b]*Centre for Obesity Research and Education (CORE), Faculty of Health and Social Care, Robert Gordon University, Garthdee Road, Aberdeen, AB10 7GJ Scotland, UK*
†Electronic supplementary information (ESI) available. See DOI: 10.1039/c6ob01850e

generation of agents with improved efficacy and solubility. In the 1990s naphthalimido compounds, such as mitonafide, were found for the first time to be highly active against cervical cancer and leukaemia cells, however, a Phase I clinical trial revealed that mitonafide treatment at doses above 118 mg m^{-2} × 5 days lead to central nervous system toxicity.[8] Subsequently, bisnaphthalimido compounds were synthesised with improved therapeutic properties. They had also overcome the dose-limiting toxicity issues,[9] however, their aqueous insolubility limited their potential use as anti-cancer agents.[10] Kong Thoo Lin and Pavlov[10] designed and synthesised a number of bisnaphthalimidopropyl derivatives, by incorporating natural polyamines and, diamino or triamino alkyl chains into the bisnaphthalimide structure. This led to improved aqueous solubility, as well as anti-cancer activity.[11,12] Additional alterations to the linker were performed to confirm that BNIP moiety was crucial for *in vitro* anti-cancer activity. One such alteration was the introduction of a bicyclohexylmethane group (in the linker chain). This tended to reduce the flexibility of the linker but it enhanced its DNA binding properties, resulting in the synthesis of BNIPDaCHM (Fig. 1). BNIPDaCHM contained a pseudo-asymmetrical centre with a mixture of three isomers (*cis*,*cis*; *trans*,*trans* and *cis*,*trans*) (indicated by asterisks, Fig. 1).[13,14] This linker chain modification resulted in a more cytotoxic BNIP derivative against triple negative breast cancer cells MDA-MB-231 (IC_{50} value 6.8 μM), compared to chemotherapy drug doxorubicin (IC_{50} value 14.4 μM), after 24 hours treatment.[13] With regards to selectivity, non-tumourigenic breast epithelial MCF-10A cells were found to be less responsive to BNIPDaCHM (IC_{50} value 6.06 μM) than doxorubicin.[13]

In the present work, we describe for the first time, the synthesis and characterisation of three novel BNIP derivatives that were designed by considering several modifications to the structure of BNIPDaCHM (Fig. 1). The first BNIP derivative, bisnaphthalimidopropyl-piperidylpropane dihydrobromide (BNIPPiProp) is a structural isomer of BNIPDaCHM that consists of only one species (enantiopure). The aim of synthesising BNIPPiProp was to investigate whether cytotoxicity and DNA binding properties differ among structural isomers and how the position of the ring structure in the linker chain affects cytotoxicity. The second BNIP derivative, bisnaphthalimidopropyl-ethylenedipiperidine (BNIPPiEth), consists of one carbon less between the two piperidine ring structures, compared to BNIPPiProp and was synthesised in order to assess the effect of a shorter linker chain on cytotoxicity and DNA binding properties. In parallel, it is still unknown whether the cytotoxicity of BNIPDaCHM is associated with the existence of the three isomers in its structure, therefore (*trans*(*trans*))-4,4′-methylenebis (cyclohexylamine), the only commercially available stereoisomer precursor required to synthesise *trans*,*trans*-BNIPDaCHM the latter being, the third BNIP derivative used in this study. The synthesis of *trans*,*trans*-BNIPDaCHM lead to the investigation into the importance of this stereoisomer compared to the mixture of three stereoisomers present in BNIPDaCHM in relation to DNA binding affinities, cytotoxicity in MDA-MB-231 and SKBR-3 breast cancer cell lines and the possible mode of cell death *via* cell cycle analysis were studied for the three novel compounds. By using two cell lines which are unresponsive to currently available anti-cancer regimes, it is possible to extend our knowledge on BNIP derivative cytotoxicity against different breast cancer cells types and to gain more information about their mode of action.

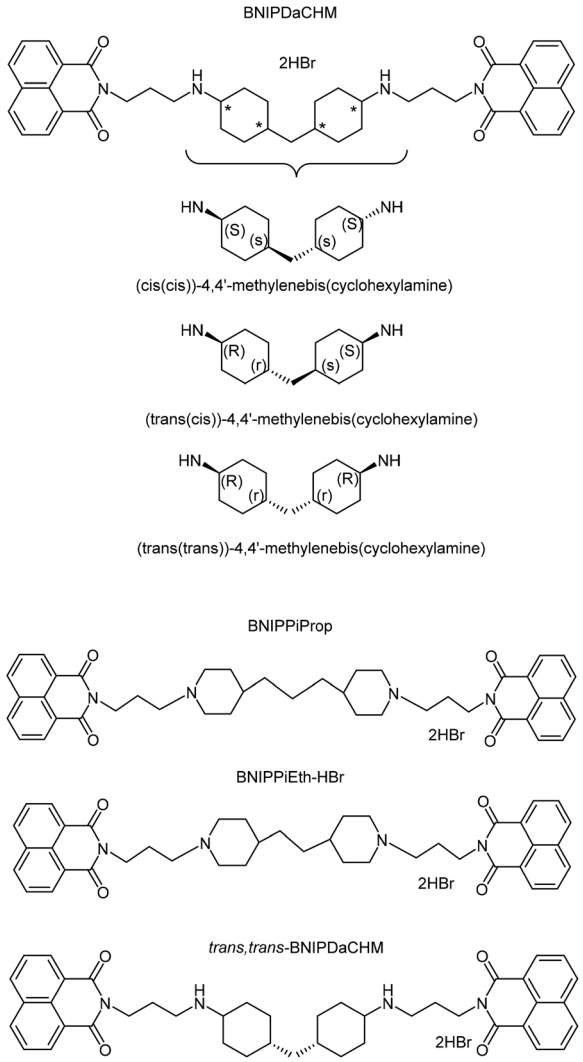

Fig. 1 Chemical structure of BNIP derivatives: BNIPDaCHM with its three stereo isomers, bisnaphthalimidopropyl-piperidylpropane (BNIPPiProp), bisnaphthalimidopropyl-ethylenedipiperidine (BNIPPiEth) and (*trans*(*trans*))-4,4′-methylenebis(cyclohexylamine) (*trans*,*trans*-BNIPDaCHM).

Results and discussion

Chemical synthesis

The synthesis of bisnaphthalimidopropyl-dipiperidyl-propane and ethane free bases was carried out by reacting 1,3-bis-(4-piperidyl) propane or 1,3-bis-(4-piperidyl)ethane and toluenesulfonyloxypropylnaphthalimide in tetrahydrofuran (THF) under reflux with subsequent addition of cesium car-

bonate (Scheme 1). The corresponding BNIPPiProp and BNIPPiEth dihydro chloride and bromide salts were prepared by their treatment with HBr/g·CH_3CO_2H and conc. HCl (72.3% and 29.5% yield), respectively.

The synthetic strategy of *trans*,*trans*-BNIPDaCHM (Scheme 2) was based on methods previously developed in our group for the synthesis of BNIPDaCHM.[13] Here the single isomer *trans*,*trans*-4,4′-methylenebiscyclohexylamine was used as the starting material. The synthesis of *trans*,*trans*-N^4,N^4-dimesityl-dicyclohexylmethane was carried out by reacting *trans*,*trans*-4,4′-methylenebis(cyclohexylamine), with 2-mesitylenesulfonyl chloride (Mts-Cl) in anhydrous pyridine (21.1% yield). *N*-Alkylation was performed by reacting *trans*,*trans*-N^4,N^4-dimesityl-dicyclohexylmethane with toluenesulfonyloxypropyl-naphthalimide in DMF (37.0% yield). For the final step, *trans*,*trans*-bisnaphthalimido-dimesityl-dicyclohexylmethane was dissolved in DCM, followed by treatment with hydrobromic acid/glacial acetic acid (HBr/g·CH_3CO_2H). All new compounds were fully characterised by NMR and high resolution mass spectrometry (see Experimental section). The melting point of *trans*,*trans*-BNIPDaCHM was found to be 120–125 °C indicating good purity. In contrast, BNIPDaCHM exhibited a

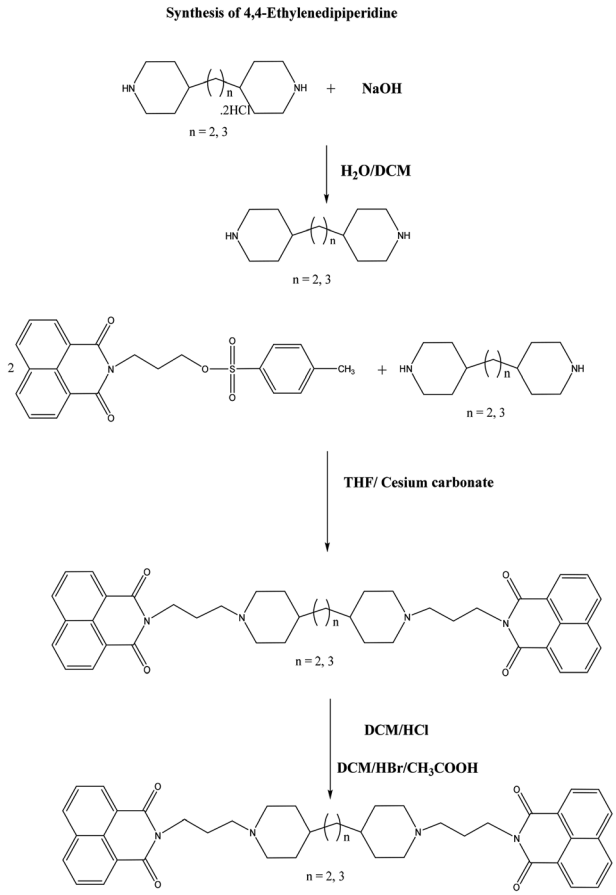

Scheme 1 Synthetic pathway of bisnaphthalimidopropyl-piperidylpropane (BNIPPiProp) and bisnaphthalimidopropyl-ethylenedipiperidine dihydrobromide (BNIPPiEth).

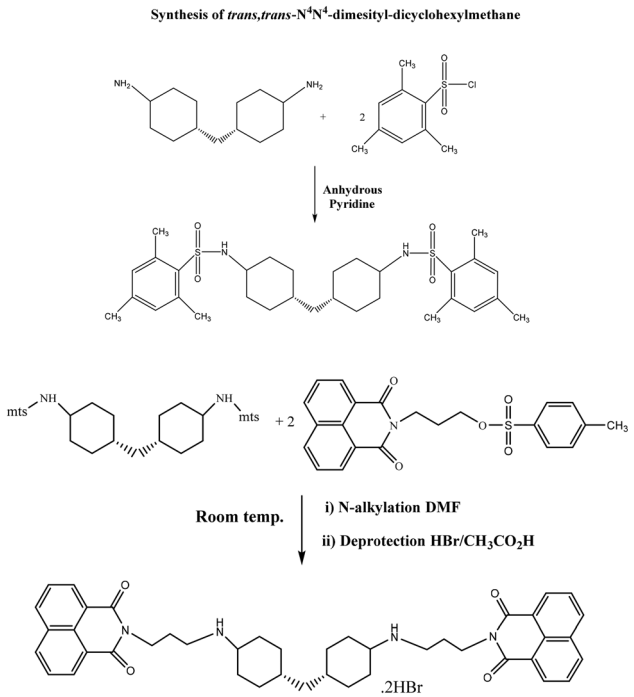

Scheme 2 Synthetic pathway of (*trans*(*trans*))-4,4′-methylenebis(cyclohexylamine) (*trans*,*trans*-BNIPDaCHM).

higher melting point range (105–130 °C) compared to *trans*,*trans*-BNIPDaCHM. BNIPPiProp and BNIPPiEth had melting points in the range of 160–170 °C and 120–125 °C, respectively, indicating their high purity.

According to matched molecular pair (MMP) analysis, which has been broadly used in the last few years to investigate the effects of hydrogen bond donors/acceptors and rotatable bonds on the melting point of drug-like compounds,[15–17] has shown that an increase in rotatable bonds leads to a decrease of the melting point.[18] Therefore, the existence of the three isomers on BNIPDaCHM increases its flexibility and leads to a low melting point, compared to the three novel compounds.

On the other hand, BNIPPiProp, with the longest linker sequence, has the highest melting point (160–170 °C), due to the increase of hydrogen bond donors/acceptors that stabilize the crystal lattice.[18]

DNA binding studies

Competitive displacement of ethidium bromide from *Calf Thymus* DNA. Competitive displacement of ethidium bromide (EtBr) with BNIPs from *Calf Thymus* DNA was carried out to investigate their DNA interactions. EtBr is a well known DNA structural probe and intercalating dye that exerts fluorescence once it binds to DNA.[19] A compound with higher DNA binding affinity than EtBr either displaces EtBr or breaks the DNA secondary structure, resulting in fluorescence quenching and a decrease in fluorescence intensity.[20] All three novel BNIP derivatives competitively displaced EtBr from *Calf Thymus* DNA duplexes. For each derivative, a range of concentrations

Table 1 Competitive displacement of EtBr from *Calf Thymus* DNA. Effect of different BNIP concentrations (0–7 μM) on % fluorescence intensity compared to *Calf Thymus* DNA alone. IC_{50} value: concentration of each BNIP derivative required to cause a 50% decrease on fluorescence intensity of DNA-EtBr complex. Data are the mean ± SD of three independent experiments (n = 3). *P < 0.05, **P < 0.01, compared to BNIPDaCHM

BNIP derivatives	Mean ± SD IC_{50} value (μM)
Calf Thymus DNA alone	–
BNIPDaCHM	2.3 ± 0.1
BNIPPiProp	3.9 ± 0.3*
BNIPPiEth	1.1 ± 0.2*
trans,*trans*-BNIPDaCHM	5.6 ± 0.2**

(0–7 μM) were tested and the corresponding IC_{50} values calculated. All BNIP derivatives displaced EtBr with IC_{50} values ranging from 1.1 to 5.6 μM confirming their high DNA binding affinity (Table 1). BNIPDaCHM was included in the following studies in order to evaluate and compare its binding properties to the novel BNIP derivatives.

The order of their binding affinity to *Calf Thymus* DNA from highest to lowest was BNIPPiEth (1.1 ± 0.2 μM), BNIPDaCHM (2.3 ± 0.1 μM), BNIPPiProp (3.9 ± 0.3 μM) and *trans*,*trans*-BNIPDaCHM (5.6 ± 0.2 μM).

BNIPPiEth, which has the shortest linker with two piperidine rings attached to an ethyl group, had the lowest IC_{50} value. The shorter length of the linker chain, as well as the incorporation of a nitrogen atom within the cyclohexane ring, compared to BNIPDaCHM, resulted in increased DNA binding. On the other hand, the incorporation of the nitrogen atom within the cyclohexane ring was not found to improve the binding properties of BNIPPiProp (3.9 ± 0.3 μM), compared to BNIPDaCHM and BNIPPiEth, confirming that the length of the bridging alkyl linkers is crucial and affects significantly BNIP binding to DNA duplexes.[21]

The *trans*,*trans*-BNIPDaCHM, a stereoisomer of BNIPDaCHM, gave a IC_{50} value of 5.6 ± 0.2 μM. BNIPDaCHM, which consists of three isomers, gave a IC_{50} value of 2.3 ± 0.1 μM, which indicated that in absence of *cis*,*cis* or/and *cis*, *trans*, *trans*,*trans*-BNIPDaCHM was not able to achieve as high DNA-binding interactions as BNIPDaCHM. Based on the above results, the planar structure of BNIPDaCHM and its mixture of three isomers was found to improve its interacting properties within the DNA base pairs, compared to *trans*,*trans*-BNIPDaCHM. This was confirmed since *trans*,*trans*-BNIPDaCHM resulted in a lower IC_{50} value compared to BNIPDaCHM, revealing that each of the three or more than one (*trans*,*trans*/*cis*,*trans* or *trans*,*trans*/*cis*,*cis*) isomers co-existing in BNIPDaCHM, are involved in the intramolecular complexes/interactions with DNA. By isolating one of its isomers (*trans*, *trans*-BNIPDaCHM), the DNA binding affinity was decreased (p < 0.01). The planar structure of BNIPDaCHM allows it to fit between the base pairs and in parallel, its rotational freedom within the plane of the aromatic rings, may allow the exposure of more than one intercalating sidechain to DNA.[22]

UV binding studies

The binding of the novel BNIP derivatives with *Calf Thymus* DNA was also studied by UV spectroscopy. A continuous decrease in UV absorption was observed at 260 nm, within the range of drug concentrations (0–7 μM) investigated. The apparent binding constants for the compounds under study, were calculated from the intercept and the slope by plotting $A_0/(A - A_0)$ against BNIP derivative concentrations,[23] where A_0 and A correspond to the absorbance values in the absence and presence of each BNIP compound (Fig. 2a), respectively. Binding constant values K for the BNIP derivatives range between 3.25 × 10^4–12.23 × 10^4 (Fig. 2b), and indicate that all BNIP derivatives interact with the DNA helix. The highest binding constant was observed with BNIPDaCHM (12.23 × 10^4), followed by *trans*,*trans*-BNIPDaCHM (11.38 × 10^4) and BNIPPiEth (10.85 × 10^4). The lowest K binding constant was observed for BNIPPiProp (3.25 × 10^4). This outcome is in agreement with the competitive displacement of EtBr studies (Table 1), highlighting the importance of linker chain length in achieving strong DNA binding interactions. In addition, the UV absorption studies revealed that *trans*,*trans*-BNIPDaCHM, the less effective derivative in displacing EtBr from DNA, obtained a high binding constant (11.38 × 10^4), compared to BNIPDaCHM (12.23 × 10^4: highest K binding constant). This suggests that *trans*,*trans*-BNIPDaCHM exhibits lower inter-

a)

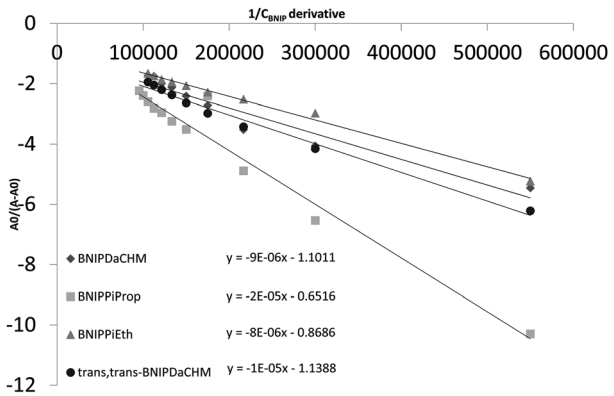

b)

BNIP derivatives	K constant
BNIPDaCHM	12.2 x 10^4
BNIPPiProp	3.3 x 10^4
BNIPPiEth	10.9 x 10^4
trans,trans-BNIPDaCHM	11.4 x 10^4

Fig. 2 (a) Competitive displacement of EtBr from *Calf Thymus* DNA. Plot of $A_0/(A - A_0)$ *versus* $1/C_{BNIP}$ of the interaction between BNIP derivatives and *Calf Thymus* DNA. (b) K constant values of BNIPP derivatives after UV binding studies.

calation capacity than the other two isomers present in the BNIPDaCHM. However, the *trans*,*trans* isomer has similar DNA affinity to the mixture of isomers present in BNIPDaCHM as demonstrated by their binding constant (Fig. 2b). Previous molecular modelling studies have revealed that for the most stable conformation of bis-1,8-naphthalimide in presence of DNA, the naphthalimide rings obtain an antiparallel orientation and are detected in the major groove.[24] Furthermore, they have been reported to induce strand cleavage, allowing the electron transfer and formation of hydrogen bonding between the nitrogen atoms and the nucleobases (excluding guanine) of the minor groove,[25] suggesting that the high *K* binding constant of *trans*,*trans*-BNIPDaCHM is obtained not only *via* intercalation, but also *via* binding on the major and minor groove of DNA.

Biological studies

Cytotoxicity. Cytotoxicity evaluation of BNIPDaCHM, BNIPPiProp, BNIPPiEth and *trans*,*trans*-BNIPDaCHM was performed by using MTT assay[26] against MDA-MB-231 and SKBR-3 cells (Table 2). After 24 hours treatment, all novel BNIP derivatives, exhibited strong cytotoxicity with IC_{50} values ranging from 1.4 μM to 3.3 μM in MDA-MB-231 cells (Table 2), compared to previously synthesised BNIPs or DNA intercalating drugs (doxorubicin) that have been tested against the same cell line, with IC_{50} values ranging from 4.9 μM to 12.7 μM.[13] In particular, *trans*,*trans*-BNIPDaCHM exhibited the lowest IC_{50} value of 1.4 μM, BNIPPiEth an IC_{50} of 1.8 μM and BNIPPiProp an IC_{50} of 3.3 μM. A similar pattern of cytotoxicity was found for SKBR-3 cells, although the IC_{50} values were between 0.2–0.7 μM (Table 2).

trans,*trans*-BNIPDaCHM (1.4 μM) was more active ($p < 0.01$) than BNIPDaCHM (2.3 μM) against MDA-MB-231 cells, showing that the existence of a single isomer in the linker sequence results in a more cytotoxic compound, compared to a compound which contains a mixture of isomers. BNIPPiEth was more cytotoxic ($p < 0.05$) than BNIPDaCHM, suggesting that the shorter length of the linker chain, as well as the incorporation of the nitrogen atom within the cyclohexane ring, not only improved the binding properties of BNIPPiEth, but enhanced significantly its *in vitro* cytotoxicity, too. Regarding BNIPPiProp, the derivative with the longest linker sequence and the highest IC_{50} value, it was found that the length of the linker chain length plays an important role in the functionality and effectiveness of a BNIP derivative. In addition, all the derivatives followed a similar pattern of cytotoxicity in both cell lines however, they appeared more cytotoxic against SKBR-3 cells. This may be due to the different mutational and tumorigenic statuses.

MDA-MB-231 cells are triple negative breast cancer cells (TNBC) (oestrogen receptor negative (ER^-), progesterone receptor negative (PR^-), human epidermal growth factor receptor 2 negative $HER2^-$) with four gene mutations being reported (BRAF, CDKN2A, KRAS and TP53) and a fast-growing basal B tumour classification (49.5% proliferation rate),[27] which makes them less responsive to anti-cancer treatments, such as docetaxel or carboplatin, compared to cells that are hormone receptor positive.[27] On the other hand, SKBR-3 cells are double negative breast cancer cells (DNBC) (ER^-, PR^-, $HER2^+$) without gene mutations and with a luminal tumour classification (35.2% proliferation rate),[27] resulting in a better response to anti-cancer treatments compared to TNBCs, which is in agreement with our findings.

Table 2 Cytotoxicity of BNIP derivatives against MDA-MB-231 and SKBR-3 cells. MDA-MB-231 and SKBR-3 cells were treated with different BNIP concentrations (0–10 μM) for 24 hours at 37 °C. IC_{50} values correspond to the concentration required to reduce cell growth by 50% compared to control cells. Data presented as mean ± SEM of 3 independent experiments ($n = 3$). *$P < 0.05$, **$P < 0.01$, compared to BNIPDaCHM

	IC_{50} values (μM)(Mean ± SEM)	
BNIP derivatives	MDA-MB-231	SKBR-3
BNIPDaCHM	2.3 ± 0.1	0.4 ± 0.1
BNIPPiProp	3.3 ± 0.1**	0.7 ± 0.1*
BNIPPiEth	1.8 ± 0.1*	0.3 ± 0.1*
trans,*trans*-BNIPDaCHM	1.4 ± 0.1**	0.2 ± 0.0*

Cell cycle analysis

Cell cycle distribution of MDA-MB-231 and SKBR-3 cells after cell synchronisation was studied using flow cytometry following PI staining[28] with the most active compound *trans*,*trans*-BNIPDaCHM (Table 2), together with BNIPDaCHM (mixture of isomers) that has been reported to induce cell cycle instability.[29]

An increase in the proportion of MDA-MB-231 cells in sub-G1 phase (122.3%, 139.3% and 142.2% increase, respectively) was exhibited relative to the control, whilst in G1 phase, the cell population was decreased after treatment with BNIPDaCHM (1 μM) and *trans*,*trans*-BNIPDaCHM (1 μM) (31.3% and 29.4% decrease, both $p < 0.05$) (Fig. 3a). The above results indicate that both BNIPDaCHM and *trans*,*trans*-BNIPDaCHM induced sub-G1 cell cycle arrest to a greater extent than camptothecin. Camptothecin is a well known positive control for sub-G1 arrest[30,31] and for inducing apoptosis.[32,33]

Therefore, this suggests that BNIPDaCHM and *trans*,*trans*-BNIPDaCHM could use similar mechanisms of action compared to camptothecin and may trigger apoptotic cell death in MDA-MB-231 and SKBR-3 human breast cancer cells.

Similar experiments were carried out with synchronised SKBR-3 cells (Fig. 3b), where the cell population was significantly increased in sub-G1 phase only after treatment with BNIPDaCHM (136.4%) and camptothecin (210.2%), but not for *trans*,*trans*-BNIPDaCHM, demonstrating that the effect of the two BNIP derivatives was different in each cell line and that the existence of one isomer has a different effect on cell cycle distribution. Therefore, it is suggested that the mechanisms of cell death among *trans*,*trans*-BNIPDaCHM and BNIPDaCHM may differ, even though they belong to the same family of compounds.

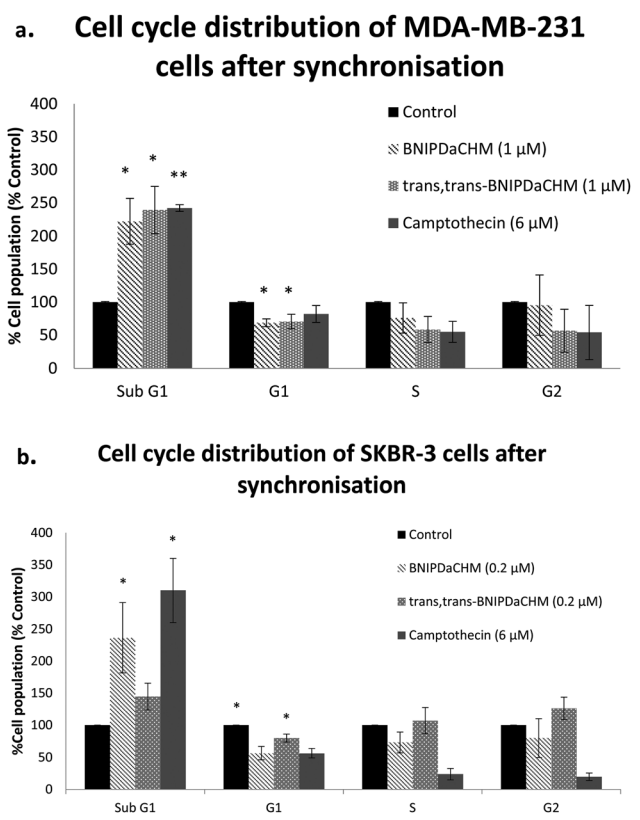

Fig. 3 Cell cycle distribution of MDA-MB-231 and SKBR-3 cells after BNIP treatment. (a) Quantification of MDA-MB-231 and (b) SKBR-3 cell cycle profiles by flow cytometry following PI staining after 24 hours treatment with BNIPDaCHM, *trans*,*trans*-BNIPDaCHM and camptothecin. DMSO/dH_2O (50% v/v) was used as the solvent control. The percentage of the cell population in sub-G1, G1, S and G2/M were calculated from histograms of linear FL-2 plots in the ungated regions (10 000 events). Data are mean ± SEM of three independent experiments (n = 3), conducted in duplicates. *P < 0.05, compared to solvent control.

Conclusions

In this study, we have shown that three BNIP derivatives, BNIPPiProp, BNIPPiEth and *trans*,*trans*-BNIPDaCHM could have potential as anti-cancer agents. DNA binding affinity was confirmed as each BNIP derivative had the ability to competitively displace EtBr from DNA and quenched UV absorption in presence of DNA in a dose dependent manner. Linker sequence modifications showed stronger cytotoxic effects against MDA-MB-231 and SKBR-3 cells, compared to the parental compound BNIPDaCHM. In addition, cell cycle analysis showed that *trans*,*trans*-BNIPDaCHM induced sub-G1 arrest in MDA-MB-231 cells, but not in SKBR-3 cells, suggesting that its mode of action could be cell line dependent, in contrast to BNIPDaCHM that shows a similar trend in cell cycle arrest in both cell lines. This study has confirmed that BNIPPiProp, BNIPPiEth and *trans*,*trans*-BNIPDaCHM have the ability to interact with DNA, intercalate and stabilise the double helix, and exhibit better cytotoxic activities, compared to previously synthesised BNIP derivatives. Further research is ongoing into the mode of DNA damage, cell death or pathway deregulations in human breast cancer cell lines.

Experimental

Chemical synthesis

BNIPPiProp, BNIPPiEth and *trans*,*trans*-BNIPDaCHM were synthesised according to the methods (with some modifications) previously described by Kong Thoo Lin and Pavlov.[10] The chemical structure, purity and stability of the derivatives were confirmed by TLC, NMR, MS and melting point determination. All reagents were purchased from Fisher Scientific or Sigma-Aldrich, unless otherwise stated. TLC was performed on silica gel 60 F254 aluminium plates (EMD/Merck) in chloroform/methanol (95 : 5). NMR was recorded on a Bruker 400 Ultrashield spectrometer operating at 400.1 MHz for ^{1}H and 100.6 MHz for ^{13}C. Accurate mass spectra were obtained by were obtained on Thermo Scientific LTQ Orbitrap XL or Waters Xevo G2-S analytical instruments (EPSRC National Mass Spectrometry Service Centre at Swansea University, Swansea).

Synthesis of bisnaphthalimidopropyl-dipiperidyl-propane base

1,3-Bis-(4-piperidyl)propane (1.19×10^{-3} mol, 0.25 g) and toluenesulfonyloxypropylnaphtalamide (2.39×10^{-3} mol, 0.98 g) were dissolved in tetrahydrofuran (THF) (6 mL). Using a reflux condenser, the reaction was stirred at 50 °C for 15 minutes and after the addition of caesium carbonate (3.069×10^{-3} mol, 1 g), the reaction was left to stir overnight at 50 °C. The reaction was monitored with TLC and once complete, the solution was poured into icy water (100 mL). A precipitate was formed and after vacuum filtration, the product was dried in a vacuum oven at 45 °C overnight. The crude product (base of BNIPPiProp) was recrystallized from ethanol and the pure product was characterised by ^{1}H-NMR (64.8% yield).

^{1}H-NMR ($CDCl_3$): δ_H 8.53–8.51 (2H, CH aromatic protons), 8.14–8.12 (2H, CH aromatic protons), 7.70–7.66 (2H, CH aromatic protons), 4.17–4.14 (2, CH_2 protons), 2.84–2.82 (2H, CH_2 protons), 2.41–2.37 (2H, CH_2 protons), 1.91–1.83 (2H, CH_2 protons), 1.79–1.74 (2H, CH_2 protons), 1.51–1.48 (2H, CH_2 protons), 1.71–1.09 (H, CH proton) ppm (parts per million).

Synthesis of BNIPPiProp salt

The base of BNIPPiProp (1.459×10^{-3} mol, 1 g) was dissolved in DCM (20 mL) and HBr/CH_3CO_2H (2 mL) was added slowly. The reaction was stirred for 2 hours at room temperature and reaction completion was monitored by TLC yielding a precipitate. The precipitate was filtered by vacuum filtration and washed with DCM (30 mL) and ether (10 mL). The BNIPPiProp salt was dried under negative pressure in a vacuum oven set at 45 °C for 2 hours (72.3% yield).

^{1}H-NMR ($CDCl_3$): δ_H 8.53–8.51 (2H, CH aromatic protons), 8.14–8.12 (2H, CH aromatic protons), 7.70–7.66 (2H, CH aromatic protons), 4.69 (2H, CH_2 protons), 4.17–4.14 (2H, CH_2 protons), 2.84–2.82 (2H, CH_2 protons), 2.41–2.37 (2H, CH_2

protons), 1.91–1.83 (2H, CH_2 protons), 1.79–1.74 (2H, CH_2 protons), 1.51–1.48 (2H, CH_2 protons), 1.71–1.09 (H, CH proton) ppm.

^{13}C-NMR ($CDCl_3$): δ_H 164.24 (C═O), 131.87 (CH aromatic), 131.60 (C aromatic), 131.24 (CH aromatic), 127.75 (C aromatic), 126.94 (CH aromatic), 122.80 (C aromatic), 56.58 (CH_2), 54.03 (CH_2), 39.10 (CH_2 aromatic), 36.77–35.69 (CH), 32.34 (CH2), 25.33 (CH_2) and 23.76 (CH_2) ppm.

Mass spectrum (HRMS), m/z = 685.3739 $(M + H)^+$ $C_{43}H_{48}N_4O_4$ requires 685.3748 $(M + H)^+$.

Synthesis of 4,4-ethylenedipiperidine

4,4-Ethylenedipiperidine dihydrochloride (7.428×10^{-4} mol, 0.2 g) was dissolved in distilled water (2 mL), sodium hydroxide (2 M, 1 mL) was added, which resulted in the formation of a precipitate. The pH was 14. The resulting was transferred into a separating funnel (100 mL) followed by extraction with DCM (300 mL). The organic layer was collected, dried with sodium sulfate and filtered. The solvent was evaporated by a rotary film evaporator. The final white solid product was left to dry under negative pressure in a vacuum oven at 45 °C for 30 minutes (90.6% yield). The synthesis of the free base was confirmed by ^{1}H-NMR.

^{1}H-NMR ($CDCl_3$): δ 2.98–2.95 (2H, CH_2 protons), 2.52–2.45 (2H, CH_2 protons), 1.8 (NH), 1.60–1.57 (2H, CH_2 protons), 1.25–1.21 (H, CH protons) and 1.19–1.16 (2H, CH_2 protons) ppm.

Synthesis of BNIPPiEth base

4,4-Ethylenedipiperidine (5.044×10^{-4} mol, 0.1 g) was reacted with toluenesulfonyloxypropyl-naphthalamide (1.001×10^{-3} mol, 0.41 g, 2.01 excess). Caesium carbonate (3.069×10^{-3} mol, 1 g) was added in the reaction. All the reagents were dissolved in THF (6 mL) and the solution refluxed overnight at 60 °C. The reaction was monitored using TLC. Once the reaction was complete, the solution was poured into icy water (100 mL), which resulting in the formation of a precipitate. The precipitate was filtered using a Buchner funnel and the product was left to dry under negative pressure in a vacuum oven at 45 °C for 60 minutes (72.3% yield). The crude product was recrystallised from ethanol and the pure product was characterised by ^{1}H-NMR.

^{1}H-NMR ($CDCl_3$): δ_H 8.52–8.50 (2H, CH aromatic protons), 8.13–8.11 (2H, CH aromatic protons), 7.69–7.65 (2H, CH aromatic protons), 4.18–4.14 (2H, CH_2 protons), 2.83–2.80 (2H, CH_2 protons), 2.40–2.36 (2H, CH_2 protons), 1.90–1.83 (2H, CH_2 protons), 1.79–1.71 (2H, CH_2 protons), 1.48 (2H, CH_2 protons), 1.2 (H, CH protons) and 1.00–0.80 (2H, CH_2 protons) ppm.

Synthesis of BNIPPiEth

BNIPPiEth (0.1 g) was dissolved in DCM (20 mL). Then, conc. HCl (1.5 mL) was added dropwise and the solution stirred at room temperature for 60 minutes, which resulted in the formation of a pale, blue precipitate. The latter was filtered and washed with ether (50 mL) and afterwards with ethanol (50 mL). The product was left under negative pressure in a vacuum oven at 45 °C for 60 minutes (29.5% yield).

^{1}H-NMR ($CDCl_3$): δ_H 8.42–8.38 (2H, CH aromatic protons), 7.82–7.78 (2H, CH aromatic protons), 4.05–4.01 (2H, CH_2 protons), 2.7 (2H, CH_2 protons), 2.44–2.43 (2H, CH_2 protons), 2.05 (2H, CH_2 protons), 1.70–1.67 (2H, CH_2 protons), 1.35–1.32 (H, CH protons) and 1.090 (2H, CH_2 protons) ppm.

^{13}C-NMR ($CDCl_3$): δ_H 164.10 (C═O), 134.81 (CH aromatic), 131.76 (C aromatic), 131.18 (CH aromatic), 127.92 (C aromatic), 127.68 (CH aromatic), 122.59 (C aromatic), 55.40 (CH_2), 52.27 (CH_2), 37.79 (CH), 29.43 (CH_2) 23.04 (CH_2) and 22.54 (CH_2) ppm.

Mass spectrum (HRMS), m/z = 671.5372 $(M + H)^+$ $C_{42}H_{46}N_4O_4$ requires 671.3592 $(M + H)^+$.

Synthesis of *N*-(3-hydroxypropyl)naphthalimide

1,8-Naphthalic anhydride (0.050 mol, 10 g) was dissolved in dimethylformamide (DMF) (140 mL). Once the 1,8-naphthalic anhydride was totally dissolved, 3-amino-1-propanol (0.050 mol, 3.75 g) and 1,8-diazabicylo[5.4.0]undec-7-ene (DBU) (13 mL) were added. The reaction was left to stir for 5 hours at 85 °C. Reaction completion was monitored with TLC and once completed; the solution was poured into icy water (200 mL) while stirring with a glass rod to form a precipitate. The precipitate was filtered and washed with water. The pure product was characterised using ^{1}H-NMR. Yield was calculated as: 53.9%.

^{1}H-NMR ($CDCl_3$): δ_H 8.66–8.63 (2H, aromatic H, doublet, J = 7.2 Hz), 8.29–8.25 (2H, aromatic H, doublet, J = 8.4 Hz), 7.83–7.78 (2H, aromatic H, doublet, J = 8.0 Hz), 4.41–4.38 (3H, triplet, J = 5.6 Hz), 3.64–3.59 (2H, CH_2, multiplet) 3.23 (OH, singlet) and 2.06–2.00 (2H, CH_2 multiplet) ppm.

Synthesis of toluenesulfonyloxypropylnaphthalimide

N-(3-Hydropropyl)naphthalimide (0.0196 mol, 5.0 g) was dissolved in anhydrous pyridine (70 mL), whilst stirring on ice. Once the *N*-(3-hydroxypropyl)naphthalimide was completely dissolved, *p*-toluenesulfonyl chloride (Ts-Cl) (0.0394 mol, 7.51 g, 2.01 excess) was slowly added to the reaction. The reaction was left at 4 °C overnight. The reaction was monitored using TLC and once it was complete, the solution was poured into icy water (200 mL) to form a precipitate which was filtered and washed thoroughly with water. The crude product was recrystallised from ethanol (68.2% yield).

^{1}H-NMR ($CDCl_3$): δ_H 8.59–8.57 (2H, aromatic H, doublet, 8.2 Hz), 8.25–8.23 (2H, aromatic H, triplet, 7.2 Hz), 7.81–7.76 (2H, multiplet), 7.30 (2H, aromatic H, doublet, 1.2 Hz), 4.27–4.20 (2H, CH_2, multiplet), 2.44 (3H, CH_3, singlet) and 2.19–2.12 (2H, CH_2, multiplet) ppm.

Synthesis of N^4,N^4-dimesityl-dicyclohexylmethane

4,4′-Methylenebis(cyclohexylamine) (4.75×10^{-3} mol, 1.0 g) was dissolved in anhydrous pyridine (10 mL) and left to stir for 15 minutes. 2-Mesitylenesulfonyl chloride (Mts-Cl) (9.56 × 10–3 mol; 2.1 g) was added. The reaction was left to stir overnight at room temperature and TLC confirmed completion of

reaction. The solution was poured into icy water (150 mL) with the formation of a precipitate. The latter was filtered by vacuum filtration, left to dry in a vacuum oven set at 45 °C for 24 hours (43.3% yield).

^{1}H-NMR ($CDCl_3$): δ_H 7.30 (NH), 6.97 (4H, CH aromatic protons), 2.99 (4H, CH protons), 2.67–2.66 (6H, CH_3-Mts protons) and 1.73–1.49 (CH_2 and cyclohexane protons) ppm.

Synthesis of protected bisnaphthalimido-dimesityl-dicyclohexylmethane

N^4,N^4-Dimesityl-dicyclohexylmethane (6.968×10^{-4} mol, 0.4 g) and toluenesulfonyloxypropylnaphthalimide (1.400×10^{-3} mol, 2.01 excess) were dissolved in DMF (8 mL). Afterwards, excess of caesium carbonate (1.13 g, 3.5×10^{-3} mol, 2.5 g excess) was added slowly. The reaction was left to stir for 48 hours at 60 °C. After TLC confirmed the reaction was complete, the solution was poured into icy water (150 mL) to form a precipitate. After vacuum filtration and several washes with water, the product was left to dry under negative filtration in a vacuum oven at 45 °C for 3 hours (92.2% yield). The product was recrystallised from ethanol and characterised by NMR.

^{1}H-NMR ($CDCl_3$): δ_H 8.50–8.47 (2H, aromatic H), 8.18–8.15 (2H, aromatic H), 7.72–7.67 (2H, aromatic H), 6.87 (2H, CH-Mts H), 6.55–6.53 (2H, CH-Mts H), 3.94–3.92 (2H, CH_2), 3.12–3.10 (2H, CH_2), 2.87–2.80 (2H, CH_2), 2.35–2.32 (3H, CH_3), 2.05–2.04 (3H, CH_3), 1.61–1.58 (H, CH), 1.61 (2H, CH_2) 1.49–1.37 (2H, CH) and 1.04 (2H, CH_2) ppm.

^{13}C-NMR ($CDCl_3$): δ_H 163.87–162.76 (C═O), 134.36 (C aromatic), 131.40–130.74 (C aromatic), 127.75 (C aromatic), 35.75 (CH_2), 30.41 (CH_2), 21.97 (CH_3) and 20.32 (CH_3) ppm.

Synthesis of bisnaphthalimidopropyl-diamino-dicyclohexylmethane dihydro-bromide salt

Bisnaphthalimido-dimesityl-dicyclohexylmethane (3.813×10^{-4} mol, 0.4 g) was dissolved in dichloromethane (DCM) (8 mL). Afterwards, hydrobromic acid/glacial acetic acid (HBr/CH_3CO_2H) (1 mL) was added drop wise. The reaction was stirred overnight at room temperature. TLC was used to confirm that the reaction was complete. The precipitate formed, was filtered by vacuum filtration and washed with DCM (15 mL) and ether (5 mL). The final product was dried under negative pressure in a vacuum oven set at 45 °C for 3 hours (37.5% yield).

^{1}H-NMR ($CDCl_3$): δ_H 8.32–8.25 (2H, aromatic Hs), 7.73–7.65 (2H, aromatic Hs), 3.70–3.64 (2H, CH_2 protons), 3.13 (2H, CH_2 protons), 2.90–2.30 (3H, CH_3 protons), 2.09–2.02 (3H, CH_3 protons), 1.83–1.80 (H, CH proton), 1.43–1.33 (2H, CH_2 protons) ppm.

^{13}C-NMR($CDCl_3$): δ 163.87–162.76 (C═O), 134.36 (C aromatic), 131.40–130.74 (C aromatic), 127.75 (C aromatic), 35.75 (CH_2) and 30.41 (CH_2) ppm.

Mass spectrum (HRMS), m/z = 685.3764 $(M + H)^+$ $C_{43}H_{48}N_4O_4$ requires 685.3748 $(M + H)^+$.

Synthesis of *trans*,*trans*-N^4,N^4-dimesityl-dicyclohexylmethane

trans,*trans*-4,4′-Methylenebis(cyclohexylamine) (2.38×10^{-4} mol, 0.05 g) was added in anhydrous pyridine (1.5 mL) and left to stir for 15 minutes with warming. After dissolution, 2-mesitylenesulfonyl chloride (Mts) (4.76×10^{-4} mol; 0.10 g) was added. The reaction was left to stir overnight at room temperature and TLC confirmed reaction completion. The solution was poured into icy water (10 mL) and stirred with a glass rod until the formation of a precipitate. The suspension was centrifuged and was washed 3 times with distilled water and the precipitate was left to dry under negative pressure in a vacuum oven set at 45 °C for overnight (21% yield). The product was afterwards characterised by 1H-NMR.

^{1}H-NMR ($CDCl_3$): δ_H 7.31 (NH), 6.98 (4H, CH aromatic protons), 3.87 (4H, CH protons), 2.67 (6H, CH_3-Mts protons), 2.33 (3H, CH_3-Mts protons), 1.84–1.82 (CH_2-cyclohexane ring), 1.65–1.62 (CH_2-cyclohexane ring), 1.16–1.10 (CH-cyclohexane ring) and 0.99–0.95 (CH_2 cyclohexane protons) ppm.

Synthesis of protected *trans*,*trans*-bisnaphthalimidopropyl-dimesityl-dicyclohexylmethane

trans,*trans*-N^4,N^4-Dimesityl-dicyclohexylmethane (6.44×10^{-5} mol, 0.037 g) and toluenesulfonyloxypropylnaphthalimide (1.29×10^{-4} mol, 0.053 g, 2.01 excess) were dissolved in DMF (1 mL). Afterwards, excess of caesium carbonate ($n = 3.07 \times 10^{-4}$ mol, 0.1 g, 5.0 excess) was added slowly. The reaction was left to stir for 48 hours at 60 °C. After TLC confirmed the reaction was complete, the solution was poured into icy water (10 mL) to form a precipitate. The suspension was centrifuged and was washed twice with distilled water. The product was left to dry under negative pressure in a vacuum oven at 45 °C for 24 hours. The crude product (59 mg, 88% yield) was purified using column chromatography and the final product (25 mg, 37% yield) was characterised by ^{1}H-NMR.

^{1}H-NMR ($CDCl_3$): δ_H 8.65–8.59 (2H, CH aromatic protons), 8.30–8.25 (2H, CH aromatic protons), 7.84–7.78 (2H, CH aromatic protons), 6.65 (4H, CH-Mts protons), 4.41–4.38 (2H, CH_2 protons), 4.06–4.04 (2H, CH_2 protons), 3.71–3.68 (2H, CH_2 protons), 2.68 (3H, CH_3 protons), 2.46–2.44 (3H, CH_3 protons), 2.34 (H, CH protons), 2.16–2.15 (2H, CH_2 protons) 1.84 (2H, CH protons) and 1.73–1.71 (2H, CH_2 protons) ppm.

^{13}C-NMR ($CDCl_3$): δ_H 141.93 (C═O), 138.76 (C aromatic), 135.17 (C aromatic), 131.95 (C aromatic), 43.72 (CH_2), 33.93–31.99 (CH_2), 23.02 (CH_3) and 20.97 (CH_3) ppm.

Synthesis of *trans*,*trans*-bisnaphthalimidopropyl-diamino-dicyclohexylmethane dihydro-bromide salt

trans,*trans*-Bisnaphthalimido-dimesityl-dicyclohexylmethane (2.38×10^{-5} mol, 25 mg) was dissolved in dichloromethane (DCM) (1.0 mL). Afterwards, hydrobromic acid/glacial acetic acid (HBr/CH_3CO_2H) (0.2 mL) was added slowly. The reaction was stirred overnight at room temperature. TLC was used to confirm that the reaction was complete. The suspension formed was transferred to Eppendorf tubes and centrifuged, was with DCM (1.0 mL) and ether (1.0 mL). The final product

was dried under negative pressure in a vacuum oven set at 45 °C for 3 hours to give the product as a white solid (8.3 mg, 41% yield).

^{1}H-NMR ($CDCl_3$): δ 8.53–8.49 (2H, CH aromatic protons), 4.16–4.12 (2H, CH aromatic protons), 3.42 (2H, CH aromatic protons) 3.04 (2H, CH_2 protons), 2.94 (2H, CH_2 protons), 2.51–2.49 (3H, CH_3 protons), 2.09–1.99 (3H, CH_3 protons), 1.75–1.72 (H, CH proton), 1.31–1.28 (2H, CH_2 protons) ppm.

^{13}C-NMR($CDCl_3$): δ 164.26 (C═O), 131.82–131.23 (C aromatic), 127.99–127.75 (C aromatic), 122.66 (C aromatic), 42.45 (CH_2) and 40.61–37.61 (CH_2) ppm.

Mass spectrum (HRMS), m/z = 685.3732 $(M + H)^+$ $C_{43}H_{48}N_4O_4$ requires 685.3748 $(M + H)^+$.

Ethidium bromide (EtBr) fluorescence displacement studies

BNIPDaCHM, BNIPPiProp, BNIPPiEth and *trans*,*trans*-BNIPDaCHM working solutions (100 μM) were prepared from stock solutions (10 mM in 50% DMSO/H_20) and were further diluted to a final concentration of 50 μM in 0.01 M saline sodium citrate (SSC) buffer. *Calf Thymus* DNA (0.5 g) was dissolved in 0.01 M SSC buffer (100 mL). EtBr solution (200 μM) was prepared by dissolving 3.94 mg of EtBr in distilled water (50 mL) and was further diluted in 0.01 SSC buffer to give the final concentration of 20 μM. Test solutions were prepared by adding varying volumes of SSC buffer, *Calf Thymus* DNA solution, EtBr solution and BNIP derivative solution. The final solutions were thoroughly mixed and analysed at 510 nm (excitation) and 520 nm (emission) using a Shimadzu RF-5301 spectrophotometer. The IC_{50} values were determined as the concentration (μM) required to decrease the fluorescence of DNA bound EtBr by 50%.

UV binding studies

BNIPDaCHM, BNIPPiProp, BNIPPiEth and BNIPDaCHM working solutions (100 μM) were prepared from their stock solutions (10 mM) as before, and were further diluted to 20 μM final concentration in 0.01 M SSC buffer. *Calf Thymus* DNA and 0.01 SSC buffer were prepared as described before (EtBr Fluorescence Displacement studies). Test solutions were prepared by adding *Calf Thymus* DNA solution (1 mL) in a quartz cuvette and BNIP derivative solution (100 μL) was added. The final solutions were thoroughly mixed and analysed at 260 nm using an Agilent 8453 UV-visible spectrophotometer. The values of apparent binding constants (K) were calculated from the intercept and slope by plotting $A_0/(A - A_0)$ against the BNIP derivative concentrations, where A_0 and A correspond to the absorbance values in absence and presence of a compound.

Cell culture maintenance

MDA-MB-231 (ECACC, Public Health England, UK, 92020424) and SKBR-3 (ATCC, HTB-30) cells were maintained in Roswell Park Memorial Institute 1640 medium (RPMI-1640) (containing GlutaMAX-1 with 25 mM HEPES), supplemented with 10% (v/v) Fetal Bovine Serum (FBS) and 1% penicillin/streptomycin (10 000 μg mL^{-1}). Cells were grown at 37 °C (5% CO_2).

Cytotoxicity

Colourimetric 3-(4,5-dimethylthiazol-2-yl)-2,5-diphenyltetrazodium bromide (MTT) assay was performed to access the growth/inhibitory effects of each BNIP compound. MDA-MB-231 and SKBR-3 cells (7.5×10^3 cells per 100 μL) were treated with different concentrations (0–10 μM) of BNIP derivatives. After 24 hours treatment, sterile-filtered MTT solution (1 mg mL^{-1}) was added to each well. After 4 hours incubation at 37 °C, the MTT solution was removed and formazan crystals solubilised in DMSO. The plates were shaken for 20 minutes at room temperature and absorbance measured at 560 nm (Synergy/HT, BIOTEK, UK). For each compound, three independent experiments were carried out and each treatment consisted of six replicates per plate. Curves were used to represent the percentage growth inhibition of MDA-MB-231 and SKBR-3 cells treated with BNIP derivatives, compared to DMSO/H_2O control that represented 100% cell viability. IC_{50} values were defined as the drug concentration that reduces absorbance compared to control values by 50%.

Cell cycle analysis

MDA-MB-231 and SKBR-3 cells (1×10^6 cells per T75 flask) cells were washed with PBS and serum free medium added in the flasks in order to achieve cell synchrony. The cells were incubated in serum free medium for 24 hours. BNIP derivatives (IC_{25} concentrations) were added and incubated for 24 hours, at 37 °C. After 24 hours treatment, the medium was removed and collected. The cells were washed twice with PBS. Both washes were collected and the cells trypsinised, mixed with the collected washes and centrifuged at 2500 rpm for 5 minutes at 4 °C. The supernatant of each sample was discarded, the pellet was resuspended in PBS (1 mL) and centrifuged at 2500 rpm for 5 minutes at 4 °C, the supernatant was discarded and the pellet resuspended in PBS (100 μL). Then, 70% (v/v) ice-cold ethanol (900 μL) was added and samples incubated for 2 hours at −20 °C. The cells were centrifuged at 5000 rpm for 5 minutes at 4 °C, the supernatant was discarded and the pellet resuspended in PBS (1 mL), followed by re-centrifugation at 5000 rpm for 5 minutes at 4 °C. The supernatant was discarded once more and the pellet resuspended in PBS (500 μL) and DNA extraction buffer (0.2 M Na_2HPO_4, 4 mM citric acid, pH 7.8, 500 μL) and incubated for 5 minutes at room temperature. The extracts were centrifuged at 5000 rpm for 5 minutes at 4 °C, the supernatant was removed and the pellets were resuspended in DNA staining solution (0.2 mg mL^{-1} Ribonuclease A (DNAse-free) and 20 μg mL^{-1} propidium iodide (PI) in PBS). The samples were incubated for 30 minutes at 4 °C in the dark and PI nuclei were examined by flow cytometry (EXPO32 ADC XL 4 color, Beckman Coulter, UK). For cell cycle analysis, EXPO32 ADC analysis software (Beckman Coulter, UK) was used to record and analyse 10 000 single events. The percentage of cells with DNA content in sub-G_1, G_1, S and G_2/M phases was calculated from histograms of linear FL-2 plots (575 nm) in the gated region.

Statistics

Three independent experiments were conducted and each experiment was comprised of at least two internal replicates. Data are presented as mean ± SD or mean ± SEM. Statistical analysis was performed by using an unpaired Student's *t*-test. Statistically significant data were detailed when $P < 0.05$).

Acknowledgements

The authors acknowledge the Robert Gordon University for financial support, and the EPSRC National Mass Spectrometry Service Centre at Swansea University, Swansea for mass spectral analysis.

References

1 R. Siegel, D. Naishadham and A. Jemal, *CA-Cancer J. Clin.*, 2013, **63**, 11–30.
2 A. Redmond, C. Byrne, F. Bane, G. Brown, P. Tibbitts, K. O'Brien, A. Hill, J. Carroll and L. Young, *Oncogene*, 2015, **34**, 3871–3880.
3 A. Becorpi, G. Sisti, F. Sorbi, E. Malosso and S. Guaschino, *Clin. Cases Miner. Bone Metab.*, 2014, **11**, 110–113.
4 B. Lehmann and J. Pietenpol, *J. Pathol.*, 2013, **232**, 142–150.
5 S. F. Chen, D. L. Behrens, C. H. Behrens, P. M. Czerniak, D. L. Dexter, B. L. Dusak, J. R. Fredericks, K. C. Gale, J. L. Gross, J. B. Jiang, M. Kirshenbau, R. J. McRipley, L. M. Papp, A. D. Patten, F. W. Perrella, S. P. Seitz, M. P. Stafford, J. H. Sun, T. Sun, M. A. Wuonola and D. D. Von Hoff, *Anti-Cancer Drugs*, 1993, **4**, 4.
6 M. F. Braña, M. Cacho, A. Gradillas, B. de Pascual-Teresa and A. Ramos, *Curr. Pharm. Des.*, 2001, **7**, 1745–1780.
7 V. Pavlov, P. Kong Thoo Lin and V. Rodilla, *Chem.-Biol. Interact.*, 2001, **137**, 15–24.
8 M. Llombart, A. Poveda, E. Forner, C. Fernández Martos, C. Gaspar, M. Muñoz, T. Olmos, A. Ruiz, V. Soriano, A. Benavides, M. Martin, E. Schlick and V. Guillem, *Invest. New Drugs*, 1992, **10**, 177–181.
9 M. F. Braña and A. Ramos, *Curr. Med. Chem.: Anti-Cancer Agents*, 2001, **1**, 237–255.
10 P. Kong Thoo Lin and V. Pavlov, *Bioorg. Med. Chem. Lett.*, 2000, **10**, 1609–1612.
11 V. Pavlov, P. Kong Thoo Lin and V. Rodilla, *Chem.-Biol. Interact.*, 2001, **137**, 15–24.
12 J. Oliveira, L. Ralton, J. Tavares, A. Codeiro-Da-Silva, C. S. Bestwick, A. MacPherson and P. Kong Thoo Lin, *Bioorg. Med. Chem.*, 2007, **15**, 541–545.
13 G. A. Barron, G. Bermano, A. Gordon and P. Kong Thoo Lin, *Eur. J. Med. Chem.*, 2010, **45**, 1430–1437.
14 R. Lima, G. A. Barron, J. Grabowska, G. Bermano, S. Kaur, N. Roy, M. Vasconcelos and P. Kong Thoo Lin, *Anti-Cancer Agents Med. Chem.*, 2013, **3**, 414–421.
15 A. Birch, P. Kenny, I. Simpson and P. Whittamore, *Bioorg. Med. Chem. Lett.*, 2009, **19**, 850–853.
16 P. Gleeson, G. Bravi, S. Modi and D. Lowe, *Bioorg. Med. Chem.*, 2009, **17**, 5906–5919.
17 P. Hajduk and D. Sauer, *J. Med. Chem.*, 2008, **51**, 553–564.
18 S. Scultes, C. de Graaf, H. Berger, M. Mayer, A. Steffen, E. Haaksma, I. de Esch, R. Leurs and O. Kramer, *MedChemComm*, 2012, **3**, 584–591.
19 P. Scaria and R. J. Shafer, *J. Biol. Chem.*, 1991, **266**, 5417–5423.
20 W. Chen, J. Turro and D. Tomalia, *Langmuir*, 2000, **16**, 15–19.
21 P. Liu, B. Wu, J. Liu, Y. Dai, Y. Wang and K. Wang, *Inorg. Chem.*, 2016, **55**, 1412–1422.
22 M. F. Braña, M. Cacho, A. Ramos, M. Dominguez, J. Pozuelo, C. Abradelo, M. Rey-Stolle, M. Yuste, C. Carrasco and C. Bailly, *Org. Biomol. Chem.*, 2003, **1**, 648–654.
23 T. Zhi-Yong, L. Jing-Hua, L. Qian, Z. Feng-Lei, Z. Zhong-Hua and W. Chao-Jie, *Molecules*, 2014, **19**, 7646–7668.
24 M. F. Braña, M. Cacho, M. Garcia, B. de Pascual-Teresa, A. Ramos, M. Dominguez, J. Pozuelo, C. Abradelo, M. Rey-Stolle, M. Yuste, M. Banez-Coronel and J. Lacal, *J. Med. Chem.*, 2004, **47**, 1391–1399.
25 C. Bailly, C. Carrasco, A. Joubert, C. Bal, N. Wattez, M. Hildebrand, A. Lansiaux, P. Colson, C. Houssier, M. Cacho, A. Ramos and M. F. Braña, *Biochemistry*, 2003, **42**, 4136–4150.
26 T. Mosmann, *J. Immunol. Methods*, 1983, **16**, 55–63.
27 P. Kenny, G. Lee, C. Myers, R. Neve, J. Semeiks, P. Spellman, K. Lorenz, E. Lee, M. Barcellos-Hoff, O. Petersen, J. Greay and M. Bissell, *Mol. Oncol.*, 2007, **1**, 84–96.
28 C. M. Henry, E. Hollville and S. J. Martin, *Methods*, 2013, **61**(2), 90–97.
29 G. A. Barron, M. Goua, I. Kuraoka, G. Bermano, S. Iwai and P. Kong Thoo Lin, *Chem.-Biol. Interact.*, 2015, **242**, 307–315.
30 C. Chu, J. Xu, D. Cheng, X. Li, S. Tong, J. Yan and Q. Li, *Mol.*, 2014, **19**(4), 4941–4955.
31 R. Doddapaneni, K. Patel and M. Singh, *Cancer Res.*, 2015, **75**(15), 2619.
32 M. Kang, J. N. Ho, H. R. Kook, S. Lee, J. J. Oh, S. K. Hong, S. E. Lee and S. S. Byun, *Oncol. Rep.*, 2016, **35**(3), 1463–1472.
33 J. U. Hong, H. J. Chung, S. Y. Bae, T. N. Trung, K. Bae and S. K. Lee, *J. Cancer Prev.*, 2004, **19**(4), 273–278.

Supplementary Material

Copies of 1H, 13C-NMR spectra and High resolution Mass Spectroscopy for three novel compounds.

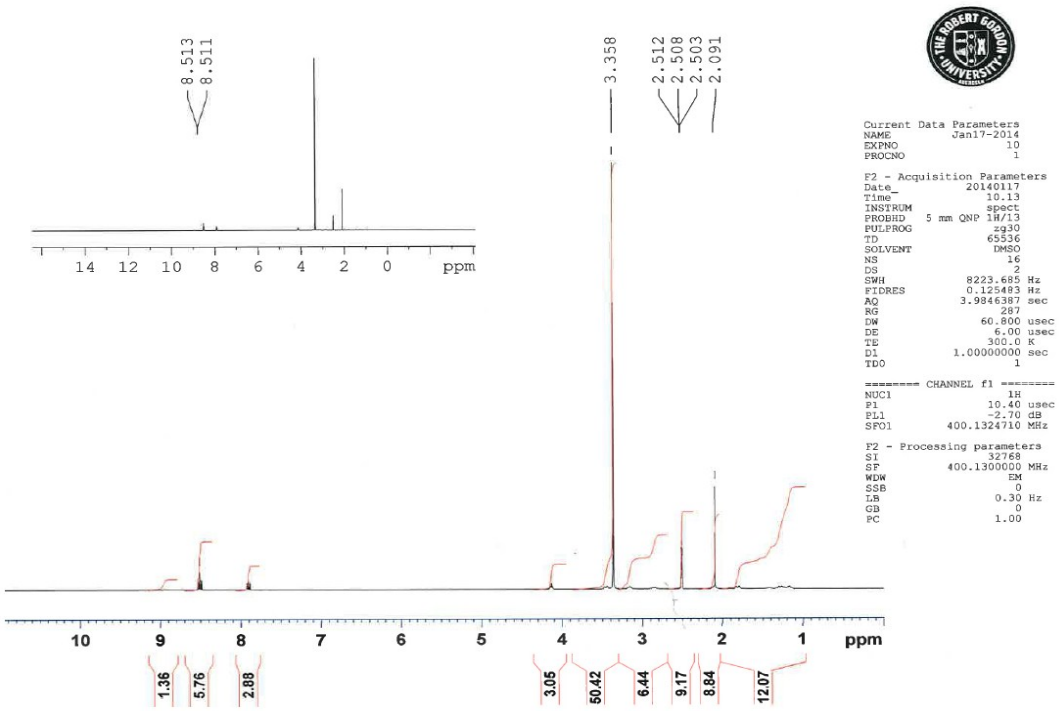

^{1}H-NMR spectrum for BNIPPiProp.

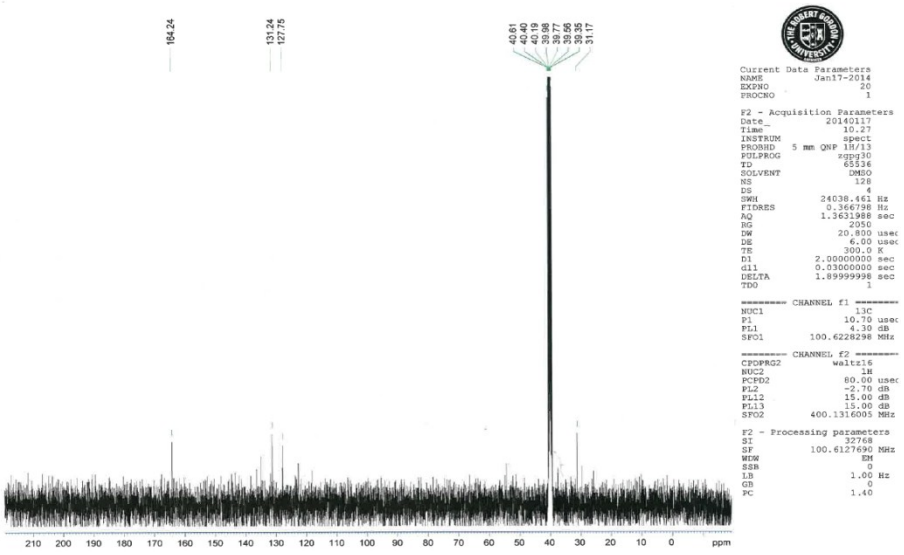

^{13}C-NMR spectrum for BNIPPiProp.

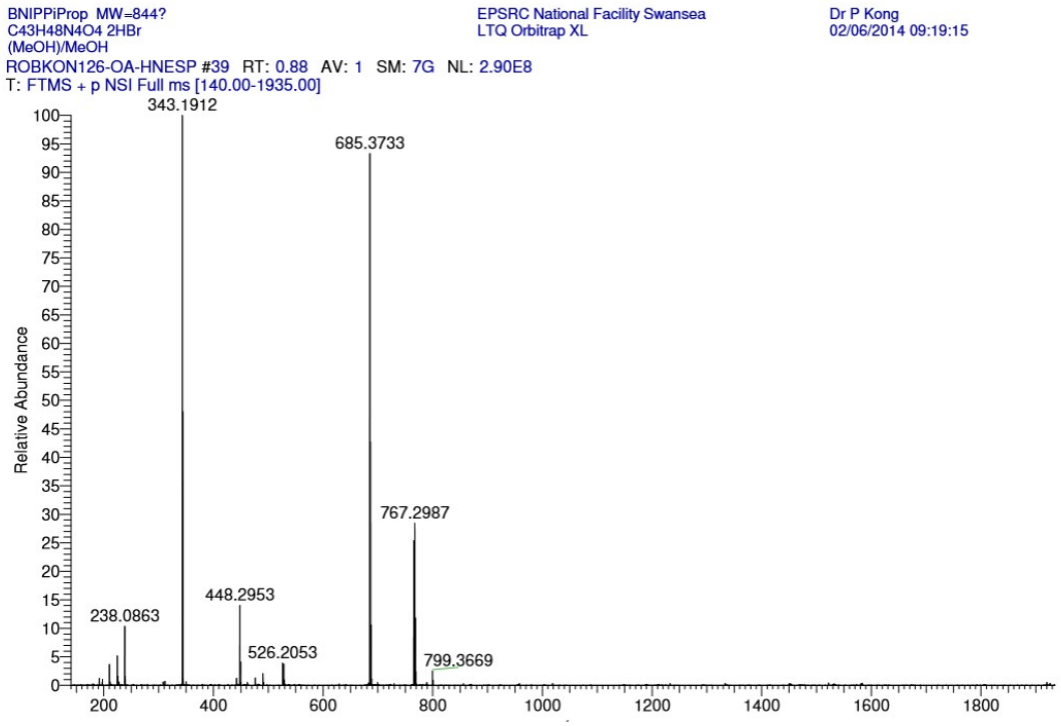

High resolution mass spectrum of BNIPPiProp.

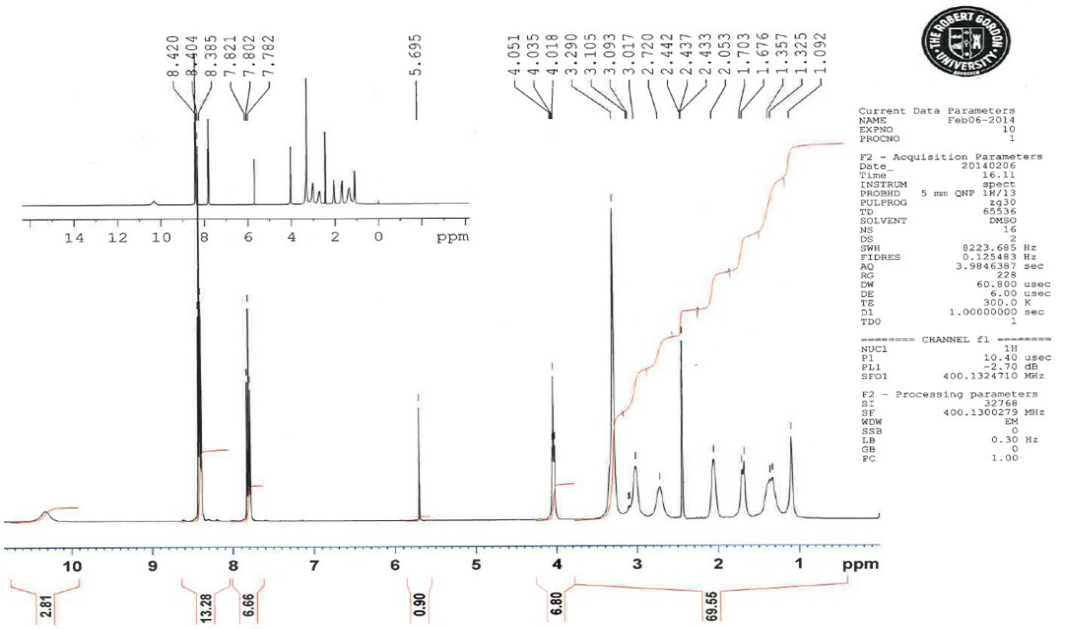

^{1}H-NMR spectrum for BNIPPiEth

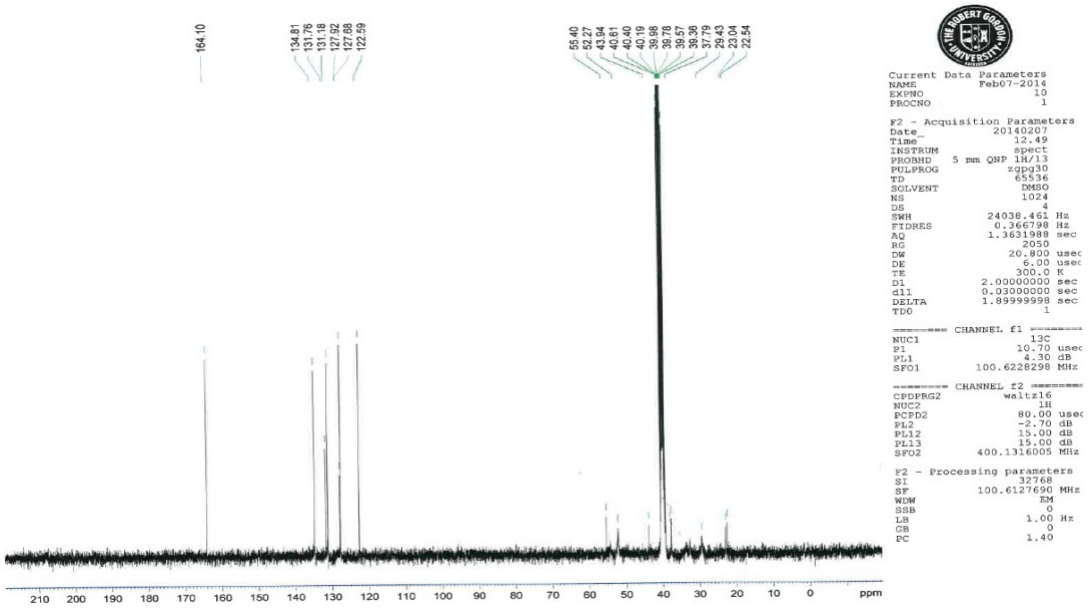

^{13}C-NMR spectrum for BNIPPiEth.

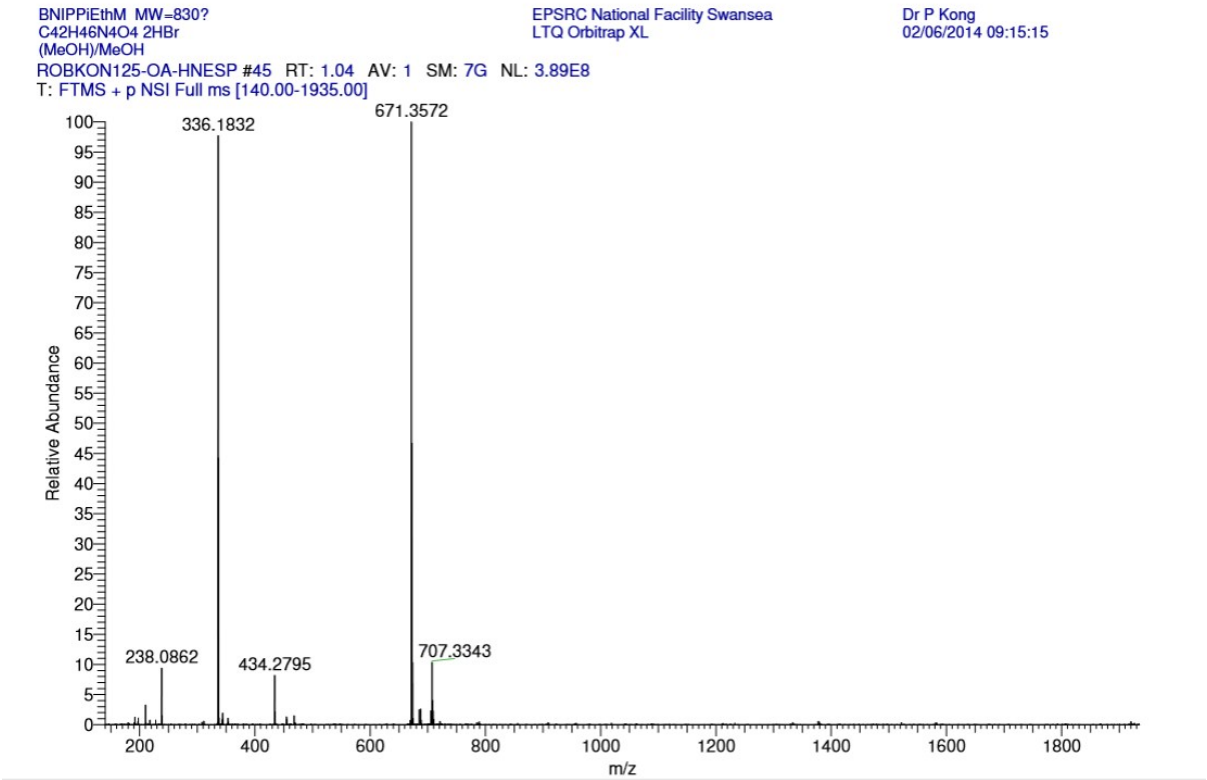

High resolution mass spectrum of BNIPPiEth.

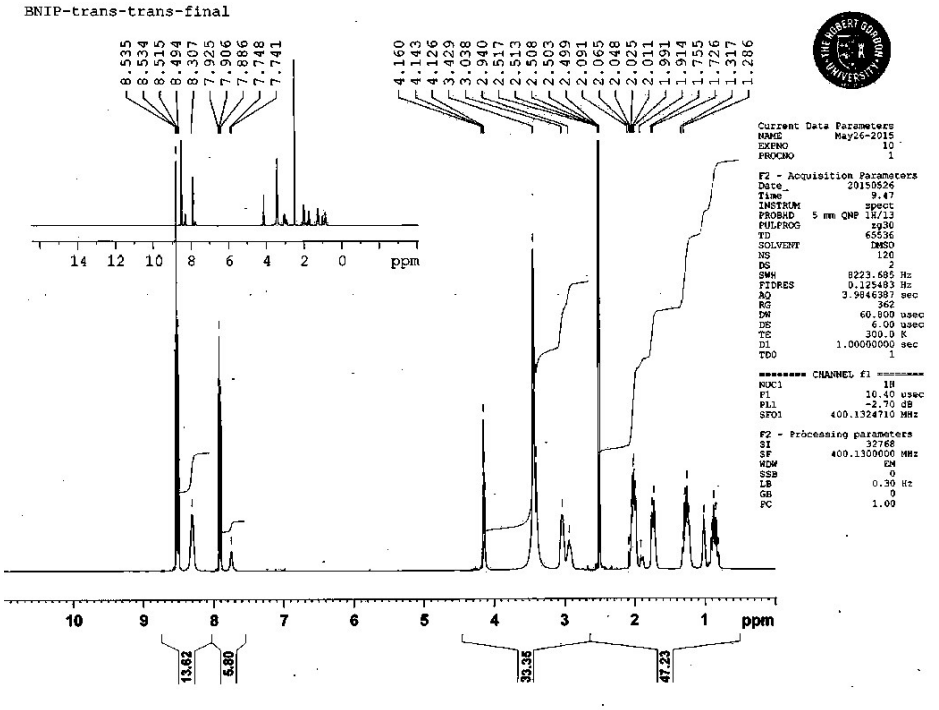

^{1}H-NMR spectrum for *trans,trans*-BNIPDaCHM.

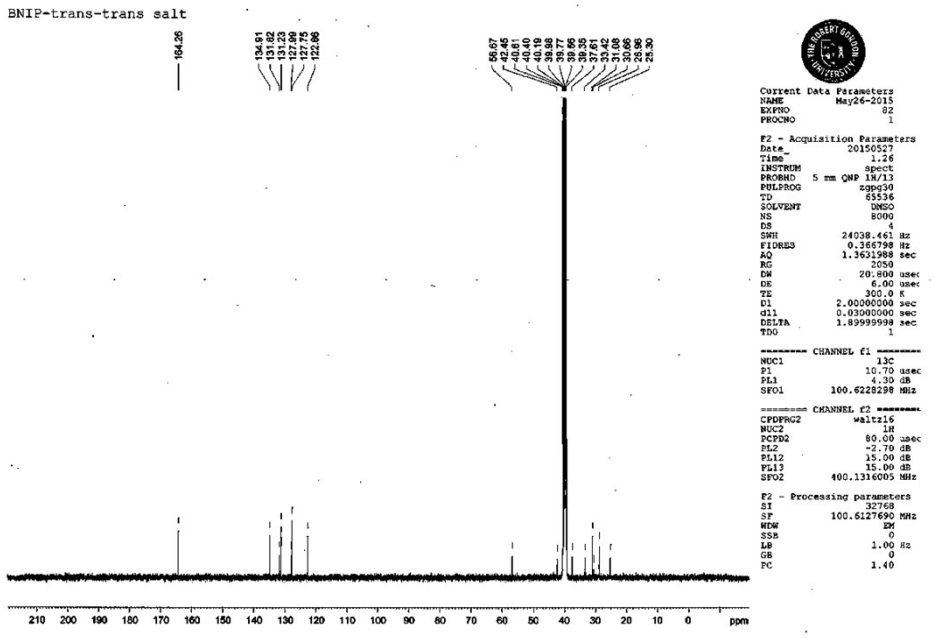

^{13}C-NMR spectrum for *trans,trans*-BNIPDaCHM.

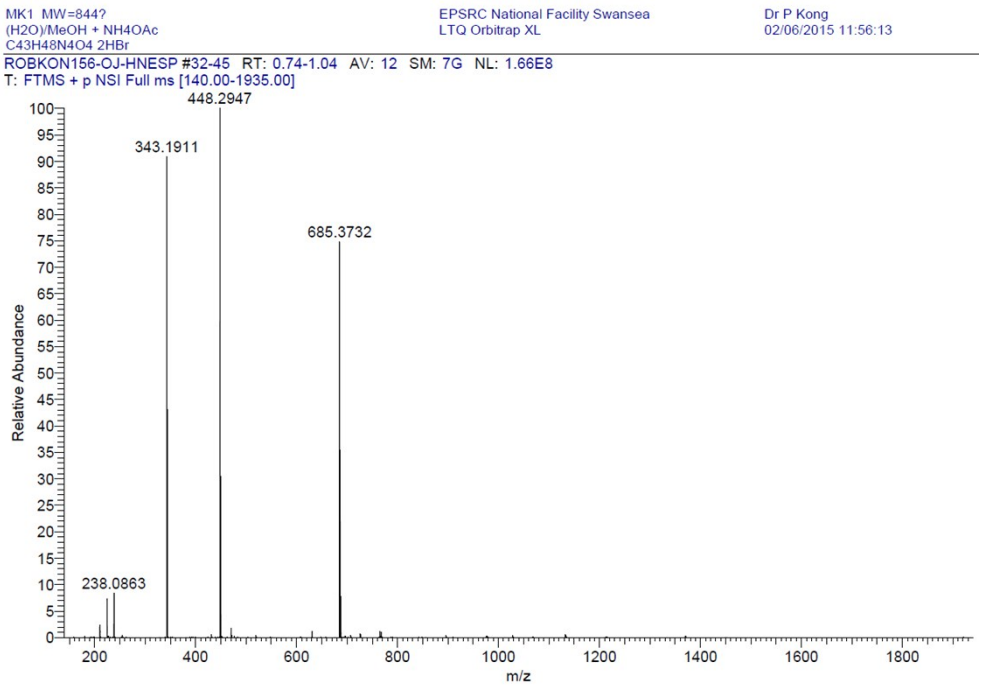

High resolution mass spectrum of *trans,trans*-BNIPDaCHM.